

Evidence for TeV gamma-ray emission from the shell type SNR RX J1713.7–3946

H. Muraishi¹, T. Tanimori², S. Yanagita¹, T. Yoshida¹, M. Moriya², T. Kifune³, S. A. Dazeley⁴, P. G. Edwards⁵, S. Gunji⁶, S. Hara², T. Hara⁷, A. Kawachi³, H. Kubo², Y. Matsubara⁸, Y. Mizumoto⁹, M. Mori³, Y. Muraki⁸, T. Naito⁷, K. Nishijima¹⁰, J. R. Patterson⁴, G. P. Rowell^{3,4}, T. Sako^{8,11}, K. Sakurazawa², R. Susukita¹², T. Tamura¹³, and T. Yoshikoshi³

¹ Faculty of Science, Ibaraki University, Mito, Ibaraki 310-8521, Japan

² Department of Physics, Tokyo Institute of Technology, Meguro, Tokyo 152-8551, Japan

³ Institute for Cosmic Ray Research, University of Tokyo, Tanashi, Tokyo 188-8502, Japan

⁴ Department of Physics and Mathematical Physics, University of Adelaide, South Australia 5005, Australia

⁵ Institute of Space and Astronautical Science, Sagami-hara, Kanagawa 229-8510, Japan

⁶ Department of Physics, Yamagata University, Yamagata 990-8560, Japan

⁷ Faculty of Management Information, Yamanashi Gakuin University, Kofu, Yamanashi 400-8575, Japan

⁸ STE Laboratory, Nagoya University, Nagoya, Aichi 464-8601, Japan

⁹ National Astronomical Observatory, Tokyo 181-8588, Japan

¹⁰ Department of Physics, Tokai University, Hiratsuka, Kanagawa 259-1292, Japan

¹¹ LPNHE, Ecole Polytechnique, Palaiseau CEDEX 91128, France

¹² Computational Science Laboratory, Institute of Physical and Chemical Research, Wako, Saitama 351-0198, Japan

¹³ Faculty of Engineering, Kanagawa University, Yokohama, Kanagawa 221-8686, Japan

Received 1 December 1999 / Accepted 23 December 1999

Abstract. We report the results of TeV gamma-ray observations of the shell type SNR RX J1713.7–3946 (G347.3–0.5). The discovery of strong non-thermal X-ray emission from the northwest part of the remnant strongly suggests the existence of electrons with energies up to ~ 100 TeV in the remnant, making the SNR a good candidate TeV gamma-ray source. We observed RX J1713.7–3946 from May to August 1998 with the CANGAROO 3.8m atmospheric imaging Čerenkov telescope and obtained evidence for TeV gamma-ray emission from the NW rim of the remnant with the significance of $\sim 5.6\sigma$. The observed TeV gamma-ray flux from the NW rim region was estimated to be $(5.3 \pm 0.9[\text{statistical}] \pm 1.6[\text{systematic}]) \times 10^{-12}$ photons $\text{cm}^{-2} \text{s}^{-1}$ at energies $\geq 1.8 \pm 0.9$ TeV. The data indicate that the emitting region is much broader than the point spread function of our telescope. The extent of the emission is consistent with that of hard X-rays observed by ASCA. This TeV gamma-ray emission can be attributed to the Inverse Compton scattering of the Cosmic Microwave Background Radiation by shock accelerated ultra-relativistic electrons. Under this assumption, a rather low magnetic field of $\sim 11\mu\text{G}$ is deduced for the remnant from our observation.

Key words: gamma-rays: observations – supernova remnant

1. Introduction

Supernova remnants (SNRs) are currently believed to be a major source of galactic cosmic rays (GCRs) from the arguments of energetics, shock acceleration mechanisms (Blandford & Eichler 1987, Jones & Ellison 1991), and the elemental abundances in the source of GCR (Yanagita et al. 1990, Yanagita & Nomoto 1999). EGRET observations suggest that the acceleration sites of GCRs at GeV energies are SNRs (Esposito et al. 1996). However, direct evidence for the SN origin of GCRs at TeV energies is scarce (e.g. Koyama et al. 1995, Allen et al. 1997, Buckley et al. 1998). Arguably the best evidence for the existence of relativistic electrons with energies around 100 TeV is the CANGAROO observation of TeV gamma-rays from the northeast rim of SN1006, which coincides with the region of maximum flux in the 2–10 keV band of the ASCA data (Tanimori et al. 1998b). This TeV gamma-ray emission was explained as arising from 2.7 K Cosmic Microwave Background Radiation (CMBR) photons being Inverse Compton (IC) up-scattered by electrons with energies up to ~ 100 TeV and allowed, together with the observation of non-thermal radio and X-ray emission, the estimation of the physical parameters of the remnant, such as the magnetic field strength (Pohl 1996, Mastichiadis 1996, Mastichiadis & de Jager 1996, Yoshida & Yanagita 1997, Naito et al. 1999).

The shell type SNR RX J1713.7–3946 was discovered in the ROSAT All-Sky Survey (Pfeffermann &

Aschenbach 1996). The remnant has a slightly elliptical shape with a maximum extent of $\sim 70'$. The 0.1–2.4 keV X-ray flux from the whole remnant is $\sim 4.4 \times 10^{-10}$ erg cm $^{-2}$ s $^{-1}$ ranking it among the brightest galactic supernova remnants. Subsequent observations of this remnant by the ASCA Galactic Plane Survey revealed strong non-thermal hard X-ray emission from the northwest (NW) rim of the remnant that is three times brighter than that from SN1006 (Koyama et al. 1997). The non-thermal emission from the NW rim dominates the X-ray emission from RX J1713.7–3946, and the SNR X-ray emission as a whole is dominated by non-thermal emission (Slane et al. 1999, Tomida 1999). It is notable that the observed emission region of hard X-rays extends over an area $\sim 0^\circ.4$ in diameter. Slane et al. (1999) carried out 843 MHz radio observations using the Molonglo Observatory Synthesis Telescope, and discovered faint emission which extends along most of the SNR perimeter, with the most distinct emission from the region bright in X-rays. Slane et al. (1999) suggest the distance to RX J1713.7–3946 is about 6 kpc based upon the observation of CO emission from molecular clouds which are likely to be associated with the remnant.

The dominance of non-thermal emission from the shell is reminiscent of SN1006. Koyama et al. (1997) proposed from the global similarity of the new remnant to SN1006 in its shell type morphology, the non-thermal nature of the X-ray emission, and apparent lack of central engine like a pulsar, that RX J1713.7–3946 is the second example, after SN1006, of synchrotron X-ray radiation from a shell type SNR. These findings from X-ray observations would suggest that TeV gamma-ray emission could be expected, as observed in SN1006, from regions in the remnant extended over an area larger than the point spread function of a typical imaging telescope ($\sim 0^\circ.2$).

Both SN1006 and RX J1713.7–3946 show notably lower radio flux densities and relatively lower matter densities in their ambient space when compared with those for the other shell type SNRs (Green 1998) for which the Whipple group (Buckley et al. 1998) and CANGAROO group (Rowell et al. 1999) have reported upper limits to the TeV gamma-ray emission. These characteristics might be related to the reason why TeV gamma-rays have been detected only for SN1006 and not from other shell type SNRs: the lower radio flux may indicate a weaker magnetic field which may result in a higher electron energies due to reduced synchrotron losses. In addition, the lower matter density would suppress the production of π^0 decay gamma-rays. An observation of TeV gamma-rays from RX J1713.7–3946 would provide not only further direct evidence for the existence of very high energy electrons accelerated in the remnant but also other important information on some physical parameters such as the strength of the magnetic field which are relevant to the particle acceleration phenomena occurring in the remnant, and would also help clarify the reason why TeV gamma-rays have until now been detected only from SN1006.

With the above motivation, we have observed RX J1713.7–3946 with the CANGAROO imaging TeV gamma-ray telescope in 1998. Here we report the result of these observations.

2. Instrument and Observation

The CANGAROO 3.8m imaging TeV gamma-ray telescope is located near Woomera, South Australia ($136^\circ 47'E$, $31^\circ 06'S$) (Hara et al. 1993). A high resolution camera of 256 photomultiplier tubes (Hamamatsu R2248) is installed in the focal plane. The field of view of each tube is about $0^\circ.12 \times 0^\circ.12$, and the total field of view (FOV) of the camera is about 3° . The pointing accuracy of the telescope is $\sim 0^\circ.02$, determined from a study of the trajectories of stars of magnitude 5 to 6 in the FOV. RX J1713.7–3946 was observed in May, June and August in 1998. During on-source observations, the center of the FOV tracked the NW rim (right ascension $17^h 11^m 56^s.7$, declination $-39^\circ 31' 52''.4$ (J2000)), which is the brightest point in the remnant in hard X-rays (Koyama et al. 1997). An off-source region having the same declination as the on-source but a different right ascension was observed before or after the on-source observation for equal amounts of time each night under moonless and usually clear sky conditions. The total observation time was 66 hours for on-source data and 64 hours for off-source data. After rejecting data affected by clouds, a total of 47.1305 hours for on-source data and 45.8778 hours for off-source data remained for this analysis.

3. Analysis and Result

The standard method of image analysis was applied for these data which is based on the well-known parameterization of the elongated shape of the Čerenkov light images using “*width*,” “*length*,” “*concentration*” (shape), “*distance*” (location), and the image orientation angle “*alpha*” (Hillas 1985, Weekes et al. 1989, Reynolds et al. 1993). However, the emitting region of TeV gamma-rays in this target may be extended, as in the case of SN1006. For extended sources, use of the same criteria as for a point source in the shower image analysis is not necessarily optimal. We made a careful Monte Carlo simulation for extended sources of various extents and found the distribution of the shower image parameter of *width*, *length*, and *concentration* for gamma-ray events is essentially the same within a statistical fluctuation as in the case of a point source. However, the simulation suggests that we should allow a wider range dependent on the extent of the source for the parameter of *distance* and *alpha* to avoid overcutting gamma-ray events. In this analysis, gamma-ray-like events were selected with the criteria of $0.^\circ 01 \leq \textit{width} \leq 0.^\circ 11$, $0.^\circ 1 \leq \textit{length} \leq 0.^\circ 45$, $0.3 \leq \textit{concentration} \leq 1.0$ and $0.^\circ 5 \leq \textit{distance} \leq 1.^\circ 2$.

Figure 1a shows the resultant *alpha* distribution when we analyzed the distribution centered at the tracking point (right ascension $17^{\text{h}} 11^{\text{m}} 56^{\text{s}}.7$, declination $-39^{\circ} 31' 52''.4$ (J2000)), which is the brightest point in the remnant in hard X-rays (Koyama et al. 1997). The solid line and the dashed line indicate the on-source and off-source data respectively. Here we have normalized the off-source data to the on-source data to take into account the difference in observation time and the variation of trigger rates due to the difference in zenith angle between on- and off-source data and due to subtle changes in weather conditions. The value of the normalization factor β is estimated to be 1.03 from the difference in total observation time for on- and off-source measurements. On the other hand, the actual value of the normalization factor β is estimated to be ~ 0.99 from the ratio of $N_{\text{on}}/N_{\text{off}}$, where N_{on} and N_{off} indicate the total number of gamma-ray-like events with *alpha* between 40° and 90° for on- and off-source data respectively. We selected the region with *alpha* $> 40^{\circ}$ to avoid any “contamination” by gamma-rays from the source, in the knowledge that the source may be extended. The small discrepancy in the two estimates of the value β might come from a slight change in the mirror reflectivity during the observation due to dew. Here we adopt the value 0.99 for β in the following analysis by taking the small discrepancy into the systematic errors due to the uncertainty in the mirror reflectivity as shown below. Figure 1b shows the *alpha* distribution of the excess events for the on-source over the off-source distribution shown in Figure 1a. A rather broad but significant peak can be seen at low *alpha*, extending to 30° . The *alpha* distributions expected for a point source and several disk-like extended sources of uniform surface brightness with various radii centered at our FOV were calculated using the Monte Carlo method. These distributions are shown in the same figure. The *alpha* distribution of the observed excess events appears to favour a source radius of $\sim 0^{\circ}.4$, which suggests the emitting region of TeV gamma-rays is extended around the NW rim of RX J1713.7–3946. The statistical significance of the excess is calculated by $(N_{\text{on}}(\alpha) - \beta N_{\text{off}}(\alpha)) / \sqrt{N_{\text{on}}(\alpha) + \beta^2 N_{\text{off}}(\alpha)}$, where $N_{\text{on}}(\alpha)$ and $N_{\text{off}}(\alpha)$ are the numbers of gamma-ray-like events with *alpha* less than α in the on- and off-source data respectively. The significance at the peak of the X-ray maximum was 5.6σ when we chose a value of *alpha* 30° considering the result of the Monte Carlo simulation shown in Figure 1b.

In order to verify this extended nature, we examined the effects of the cut in shape parameters on the *alpha* distribution by varying each cut parameter over wide ranges. We also produced *alpha* distributions for different energy ranges and data sub-sets. Similar broad peaks in the *alpha* distribution persisted through these examinations. Also we examined more recent data from PSR1706–44 from July and August 1998 and obtained a narrow peak at *alpha* $< 15^{\circ}$, as expected for a point source. This confirms that the extended nature of the TeV gamma-ray emitting

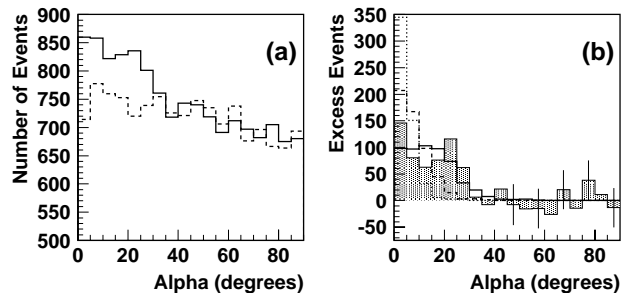


Fig. 1. (a) Distributions of the orientation angle “*alpha*” for gamma-ray-like events with respect to the center of the field of view, which for on-source data corresponds to the NW rim of RX J1713.7–3946. The solid line and dashed line are for on-source and off-source data respectively. (b) Distribution of the excess events of the on-source over the off-source level shown in Figure 1a, shown as the shaded bins. The vertical bars for several bins indicate plus and minus one standard deviation which is approximately the same for all bins. The expected *alpha* distribution for a point source (dotted line), and disk-like sources with a radius of $0^{\circ}.2$ (dashed line) and $0^{\circ}.4$ (thick solid line) centered at the FOV by the Monte Carlo method are also shown. Here the curves are normalized to the actual excess number of gamma-ray-like events with *alpha* $\leq 30^{\circ}$.

region does not come from some malfunction of our telescope system and/or systematic errors in our data analysis. A similar, but not as broad, *alpha* peak was seen for SN1006 (Tanimori et al. 1998b).

In order to see the extent of the emitting region, we made a significance map of the excess events around the NW rim of RX J1713.7–3946. Significances for *alpha* $\leq 30^{\circ}$ were calculated at all grid points in $0^{\circ}.1$ steps in the FOV. Figure 2 shows the resultant significance map of the excess events around the NW rim of RX J1713.7–3946 plotted as a function of right ascension and declination, in which the contours of the hard X-ray flux (Tomida 1999) are overlaid as solid lines. The solid circle indicates the size of the point spread function (PSF) of our telescope which is estimated to have a standard deviation of $\sim 0^{\circ}.25$ for *alpha* $\leq 30^{\circ}$ based upon Monte Carlo simulations for a point source with a Gaussian function. The area which shows the highest significance in our TeV gamma-ray observation coincides almost exactly with the brightest area in hard X-rays. The region which shows the emission of TeV gamma-rays with high significance ($\geq 3\sigma$ level) extends wider than our PSF and appears to coincide with the ridge of the NW rim that is bright in hard X-rays. It extends over a region with a radius of $\sim 0^{\circ}.4$. This region persisted in similar maps calculated for several values of *alpha* narrower than 30° .

The integral flux of TeV gamma-rays was calculated, assuming emission from a point source, to be $(5.3 \pm 0.9$ [statistical] ± 1.6 [systematic]) $\times 10^{-12}$ photons $\text{cm}^{-2} \text{s}^{-1}$ ($\geq 1.8 \pm 0.9$ TeV). The flux value and the statistical error were estimated from the excess number of $N_{\text{on}}(30^{\circ}) - \beta N_{\text{off}}(30^{\circ})$, where the value of 30° for *alpha*

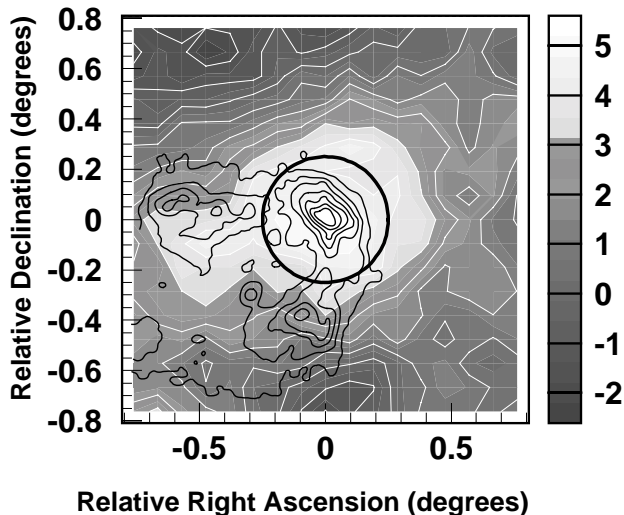


Fig. 2. Contour map of significance around the NW rim of RX J1713.7–3946 centered at the region brightest in hard X-ray emission (right ascension $17^{\text{h}} 11^{\text{m}} 56^{\text{s}}.7$, declination $-39^{\circ} 31' 52''.4$ (J2000)). White lines indicate the significance level. The contours of the 0.5–10 keV band of the X-ray flux (from Tomida 1999) also are overlaid as solid lines. The solid circle indicates the size of our PSF.

is chosen by the argument mentioned before. The causes of the systematic errors are categorized by uncertainties in (a) assumed differential spectral index, (b) the loss of gamma-ray events due to the parameter cuts, (c) the estimate of core distance of showers by the Monte Carlo method, (d) the trigger condition, (e) the conversion factor of the ADC counts to the number of photo-electrons, and (f) the reflectivity of the reflector. These errors from (a) to (f) are estimated as 15%, 22%, 3%, 12%, 10%, and 8% for the integral flux and 24%, 2%, 8%, 20%, 29%, and 17% for the threshold energy, respectively. The total systematic errors shown above are obtained by adding those errors quadratically.

To summarise, all our observed data support the hypothesis that the emitting region of the NW rim is extended. In general, the value of the effective detection area of the telescope system for extended sources would be reduced by some factor from that for a point source, because the gamma-ray detection efficiency decreases with the distance of emitting points from the center of the FOV when we observe with a single dish. We calculated the efficiency as a function of the distance by the Monte Carlo method by analyzing the data with the same criteria as applied to the actual data. We estimated the value of the correction factor to the effective area to be ~ 1.2 for our target by integrating the efficiency over the distance for an extended disk-like source of uniform surface brightness with a radius of $0^{\circ}.4$. The factor of 1.2 is less significant than the systematic errors estimated above.

4. Discussion

The SNR RX J1713.7–3946 is reminiscent of SN1006 both in the synchrotron X-ray emission from the shell far from the centre of the remnant and also in the TeV gamma-ray emission from an extended region coincident with that of the non-thermal X-rays. This suggests that the particles responsible for the emission of the high energy photons are accelerated in shocks.

There are several possible emission processes of TeV gamma-rays: the emission induced by accelerated protons (by the π^0 decay process) and by electrons – through bremsstrahlung and/or the Inverse Compton (IC) process. The expected integral flux of gamma-rays above our threshold energy of ~ 1.8 TeV by the π^0 decay process is estimated to be $< 4 \times 10^{-14}$ photons $\text{cm}^{-2} \text{s}^{-1}$ (Drury et al. 1994, Naito & Takahara 1994), where we assume the distance and the upper limit for the number density in the ambient space of the remnant as 6 kpc and 0.28 atoms/ cm^3 , respectively (Slane et al. 1999). This flux value is too low to explain our observed flux, even taking into account the large uncertainties in the estimates of the distance and the ambient matter density of the remnant (Slane et al. 1999, Tomida 1999). However, there remains the possibility of some contribution of the π^0 decay process if the remnant is interacting with a molecular cloud located near the NW rim (Slane et al. 1999). The relative contribution in emissivity of the bremsstrahlung process compared to π^0 decay process is estimated as $\sim 10\%$, assuming the flux ratio of electrons to protons is $\sim 1/100$ and that both have power law spectra with the index of 2.4 (Gaisser 1990), indicating this process is also unlikely to dominate. Therefore, the most likely process for TeV gamma-ray emission seems to be the IC process.

Under this assumption, the magnetic field strength in the supernova remnant can be deduced from the relation $L_{\text{syn}}/L_{\text{IC}} = U_{\text{B}}/U_{\text{ph}}$ between the IC luminosity L_{IC} and synchrotron luminosity L_{syn} , where $U_{\text{B}} = B^2/8\pi$ and U_{ph} are the energy densities of the magnetic field and the target photon field, respectively. L_{syn} and L_{IC} in the above formula must be due to electrons in the same energy range. The value of L_{syn} which should be compared with our TeV gamma-ray data is estimated from the ASCA result to be $L_{\text{syn}} = L_{\text{ASCA}} \int_{E_{\text{syn}}^{\text{min}}}^{\infty} E^{-1.44} dE / \int_{0.5\text{keV}}^{10\text{keV}} E^{-1.44} dE$, extrapolating the synchrotron spectrum with the same power law out of the energy range of 0.5–10 keV covered by ASCA (Tomida 1999). Here $L_{\text{ASCA}} = 2.0 \times 10^{-10}$ erg $\text{cm}^{-2} \text{s}^{-1}$ is the X-ray luminosity in the 0.5–10 keV energy band observed by ASCA from the NW rim of the remnant and the power law index of -1.44 is the mean value for index of X-rays in the same energy range (Tomida 1999). $E_{\text{syn}}^{\text{min}} = 0.14(B/10\mu\text{G})$ keV is a typical synchrotron photon energy emitted by electrons which emit 1.8 TeV photons (the threshold energy of our observation) by the IC process when we assume the target photons to be from the CMBR. The value of L_{IC} is calculated to be 4.2×10^{-11}

erg cm⁻² s⁻¹ from our result for the number of photons of TeV gamma-rays, and using the fact that the spectra of synchrotron photons and IC photons follow the same power law when the electrons have a power law spectrum. Thus inserting L_{syn} , L_{IC} , and $U_{\text{ph}} = 4.2 \times 10^{-13}$ erg cm⁻³ of the energy density for the CMBR into the above relation, we can solve for the magnetic field strength B . Finally, the magnetic field at the NW rim is estimated to be $\sim 10.8 \mu\text{G}$. The extrapolation used to estimate L_{syn} is reasonable, because $E_{\text{syn}}^{\text{min}}$ is estimated to be 0.15 keV; this is not so different from the minimum energy of the ASCA band (0.5 keV).

The electrons responsible for the synchrotron and IC photon emissions are likely to have been accelerated by the shocks in the remnant as discussed above. If the maximum electron energy is limited by synchrotron losses, this maximum energy can be estimated by equating the cooling time due to synchrotron losses with the time scale of acceleration by the first Fermi process in a strong shock as $\sim 50(V_s/2000\text{km s}^{-1})(B/10\mu\text{G})^{-0.5}$ TeV, where V_s is the shock velocity (Yoshida & Yanagita 1997). On the other hand, equating the acceleration time with the age of the remnant, the maximum energy can be expressed $\sim 180(V_s/2000\text{km s}^{-1})^2(B/10\mu\text{G})(t_{\text{age}}/10000\text{year})$ TeV. In either case, whether it is synchrotron losses or the age of the remnant that limits the maximum electron energy (Reynolds & Keohane 1999), electrons should exist with energies high enough to emit the observed synchrotron X-rays and TeV gamma-rays by the IC process.

It is notable that both RX J1713.7–3946 and SN1006 have relatively low magnetic field strengths and low matter densities in their ambient space. These common features may have arisen if the magnetic field was ‘frozen in’ to the matter without amplification other than by compression by shocks and may be the reason why electrons are accelerated to such high energies. These facts may also explain the radio quietness (Green 1998) and the weak emissivity of π^0 decay gamma-rays of the remnants. For SN1006, the low matter density in the ambient space might result from the remnant being located far off the galactic plane and the supernova being of type Ia. For RX J1713.7–3946, the low matter density may be caused by material having been swept out by the stellar wind of the supernova progenitor (Slane et al. 1999). The low magnetic field and the low matter density in the ambient space of SN1006 and RX J1713.7–3946 may explain why TeV gamma-rays have been detected so far only for these two remnants.

In conclusion, we have found evidence for TeV gamma-ray emission from RX J1713.7–3946 at the level of 5.6 sigma. If confirmed (à la Weekes 1999), this would be the second case after SN1006 to show directly that particles are accelerated up to energies of ~ 100 TeV in the shell type SNR.

Acknowledgements. We sincerely thank H. Tomida and K. Koyama for providing us the ASCA data. We thank the referee very much for his helpful comments on the paper. This work is supported by a Grant-in-Aid for Scientific Research from Japan’s Ministry of Education, Science, and Culture, a grant from the Australian Research Council and the (Australian) National Committee for Astronomy (Major National Research Facilities Program), and the Sumitomo Foundation. The receipt of JSPS Research Fellowships (SH, AK, GPR, KS, and TY) is also acknowledged.

References

- Allen, G. E., et al., 1997, ApJ 487, L97
 Blandford, R. D. & Eichler, D., 1987, Phys. Rep. 154, 1
 Buckley, J. H., et al., 1998, A&A 329, 639
 Drury, L. O’C., et al., 1994, A&A 287, 959
 Esposito, J. A., et al., 1996, ApJ 461, L820
 Gaisser, T. K., 1990, Cosmic Rays and Particle Physics, Cambridge University Press
 Green, D. A., 1998, A Catalogue of Galactic Supernova Remnants (1998 September version), Mullard Radio Astronomy Observatory, Cambridge, UK (<http://www.mrao.cam.ac.uk/surveys/snrs/>)
 Hara, T., et al., 1993, Nucl. Instr. Meth. Phys. Res. A 332, 300
 Hillas, A. M., 1985, Proc. 19th Int. Cosmic Ray Conf. (La Jolla) 3, 445
 Jones, F. C. & Ellison, D. C., 1991, Space Sci. Rev. 58, 259
 Koyama, K., et al., 1995, Nature 378, 255
 Koyama, K., et al., 1997, PASJ 49, L7
 Mastichiadis, A., 1996, A&A 305, L53
 Mastichiadis, A. & de Jager, O.C., 1996, A&A 311, L5
 Naito, T. & Takahara, F., 1994, J. Phys. G 20, 477
 Naito, T., et al., 1999, submitted to Astron. Nachr.
 Pfeffermann, E. & Aschenbach, B., 1996, in ‘Roentgenstrahlung from the Universe’, MPE Report 263, P267
 Pohl, M., 1996, A&A 307, 57
 Reynolds, P. T., et al., 1993, ApJ 404, 206
 Reynolds, S. P. & Keohane, J. W., 1999, ApJ 525, 368
 Rowell, G. P., et al., 1999, submitted to A&A
 Slane, P., et al., 1999, ApJ 525, 357
 Tanimori, T., et al., 1994, ApJ 429, L61
 Tanimori, T., et al., 1998b, ApJ 497, L25
 Tomida, H., 1999, Ph. D. thesis, Kyoto Univ. (unpublished)
 Yanagita, S., Nomoto, K., and Hayakawa, S., 1990, Proc. 21st Int. Cosmic Ray Conf. (Adelaide) 4, 44
 Yanagita, S. & Nomoto, K., 1999, Proc. 3rd INTEGRAL Workshop ‘The Extreme Universe’ in press, Astrophys. Letters & Communications
 Yoshida, T. & Yanagita, S., 1997, Proc. 2nd INTEGRAL Workshop ‘The Transparent Universe’ ESA SP-382, 85
 Weekes, T.C., et al., 1989, ApJ 342, 379
 Weekes, T.C., 1999, astro-ph/9910394, to appear in ‘GeV-TeV Astrophysics: Toward a Major Atmospheric Cherenkov Telescope VI,’ Snowbird, Utah